BAMS Article

# Perspectives on Sea- and Lake-Effect Precipitation from Japan's "Gosetsu Chitai"

W. James Steenburgh and Sento Nakai

**ABSTRACT:** A remarkable snow climate exists on the Japanese islands of Honshu and Hokkaido near the Sea of Japan. Mean annual snowfall in this "gosetsu chitai" (heavy snow area) exceeds 600 cm (235 in.) in some near-sea-level cities and 1,300 cm (512 in.) in some mountain areas. Much of this snow falls from December to February during the East Asian winter monsoon when frequent cold-air outbreaks occur over the Sea of Japan. The resulting sea-effect precipitation systems share similarities with lake-effect precipitation systems of the Laurentian Great Lakes of North America, but are deeper, are modulated by the regional coastal geometry and topography, and can sometimes feature transversal mode snowbands. Snowfall can maximize in the lowlands or the adjoining mountains depending on the direction and strength of the boundary layer flow. Remarkable infrastructure exists in Japan for public safety, road and sidewalk maintenance, and avalanche mitigation, yet snow-related hazards claim more than 100 lives annually. For winter recreationists, there is no surer bet for deep powder than the mountains of Honshu and Hokkaido near the Sea of Japan in January, but the regional snow climate is vulnerable to global warming, especially in coastal areas. Historically, collaborative studies of sea- and lake-effect precipitation systems involving North American and Japanese scientists have been limited. Significant potential exists to advance our understanding and prediction of sea- and lake-effect precipitation based on studies from the Sea of Japan region and efforts involving meteorologists in North America, Japan, and other sea- and lake-effect regions.



**AFFILIATIONS: Steenburgh**—Department of Atmospheric Sciences, University of Utah, Salt Lake City, Utah; **Nakai**—Snow and Ice Research Center, National Research Institute for Earth Science and Disaster Resilience, Nagaoka, Japan

https://doi.org/10.1175/BAMS-D-18-0335.1

Corresponding author: Dr. W. James Steenburgh, jim.steenburgh@utah.edu

In final form 23 September 2019

Portions of Honshu and Hokkaido Islands of Japan experience remarkable snowfalls during the East Asian winter monsoon when frequent cold-air outbreaks occur over the Sea of Japan (also known as the East Sea) (Magono et al. 1966; Tsuchiya and Fujita 1967; Yoshino 1977; Hozumi and Magono 1984; Nakai et al. 1990; Nakai et al. 2003, 2005; Eito et al. 2010). Within this densely populated "gosetsu chitai" (heavy snow area), Joetsu (population: 197,000) on the west coast of central Honshu, Aomori (population: 314,000) on the north coast of Honshu, and Sapporo (population: 1.95 million) on the west coast of Hokkaido average 635 cm (250 in.), 669 cm (263 in.), and 597 cm (235 in.) of annual snowfall, respectively (Japan Meteorological Agency 1981–2010 normals; see Fig. 1 for geographic locations). Mean annual snowfall in the adjacent mountains can exceed 1,300 cm (512 in.). Snow depths can reach 2 m near sea level and 7 m in the mountains (Yamaguchi et al. 2011), with the snow corridor along the Tateyama Kurobe Alpine Route in the Hida Mountains (aka northern Japanese Alps) famous for its towering snow walls when it opens each spring (Fig. 2). While snowfall is most prolific in Japan, some coastal areas of Korea, Russia, and China observe less frequent but high-impact snowstorms produced by the Sea of Japan or the Yellow Sea (Zhou et al. 2008; Yang et al. 2009; Jung et al. 2012; Nam et al. 2014; Podolskiy et al. 2014; Bao and Ren 2018).

An extensive body of literature examining sea-effect precipitation and its climatic and societal impacts in Japan and East Asia exists, but is often overlooked by North American meteorologists. For example, of 85 articles in the AMS Journals Online with "lake effect" or "lake-effect" in the title, 83 include the phrase "Great Lakes," but only 23 include the word "Japan." Although there are exceptions such as the 1993 Study of Precipitation Formation in Snow Clouds and Feasibility of Snow Cloud Modification by Seeding, which involved the University of Wyoming King Air (Murakami et al. 2003; Murakami 2019), collaborations between Japanese and North American scientists investigating

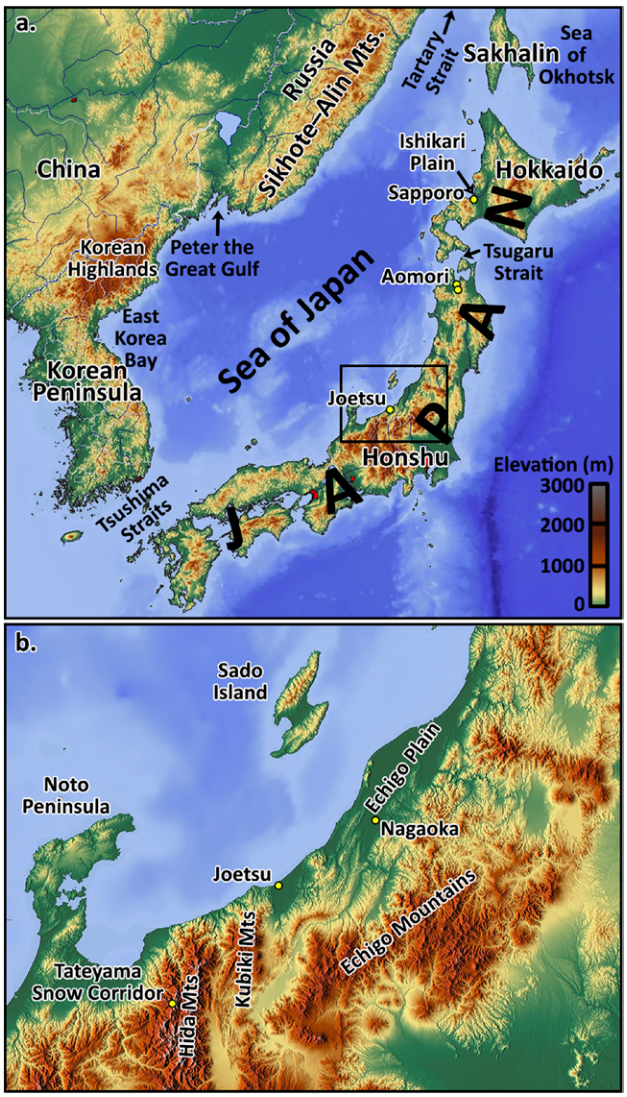


Fig. 1. Major topographic and geographic features of (a) the Sea of Japan region and (b) central Honshu near the Sea of Japan. Elevation (m) shaded following scale in (a).

Fig. 2. The snow corridor along the Tateyama Kurobe Alpine Route. [Source: Uryah, Wikipedia Commons, CC BY-SA 3.0.]

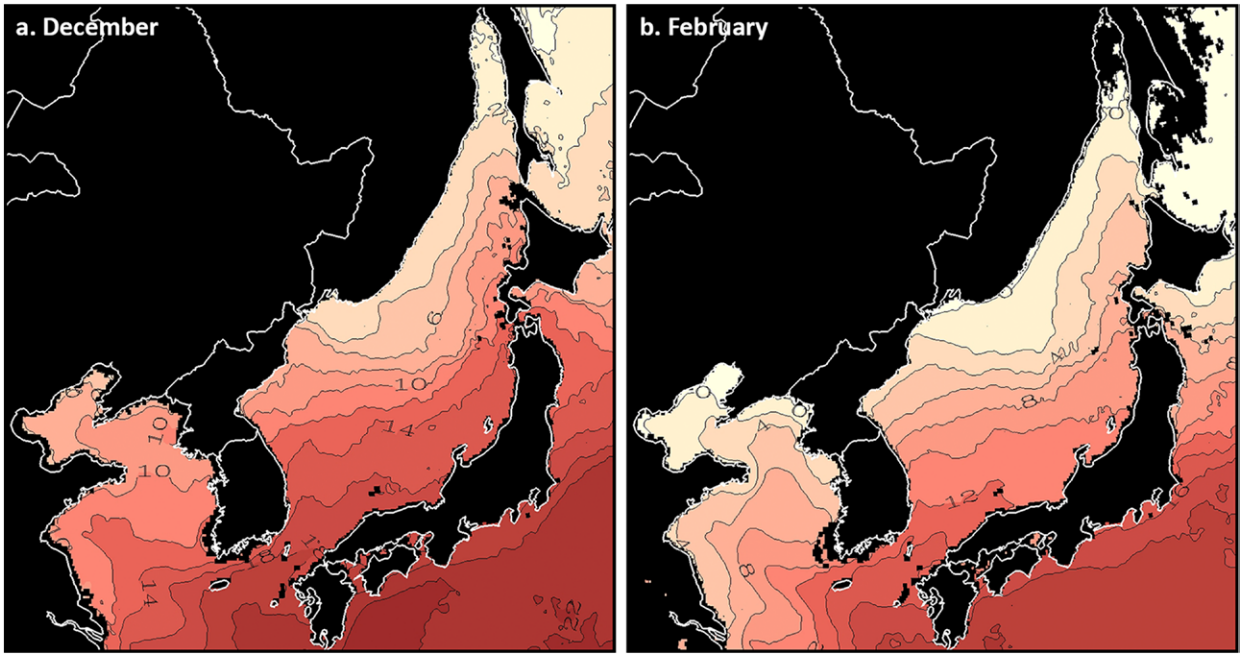


**Fig. 3. GMIS-Pathfinder monthly mean SST (color-filled contours every 2°C, smoothed with a 9-point smoother for clarity) in (a) December and (b) February. Data described by Melin (2013).**

sea- and lake-effect precipitation have been limited historically. In this paper, we seek to introduce North American meteorologists to the snow climate of western Japan, summarize contemporary knowledge concerning sea-effect precipitation generated by the Sea of Japan, and stimulate increased collaborations between sea- and lake-effect researchers and forecasters in North America, Japan, East Asia, and other regions of the world.

## The Sea of Japan region and climate

The Sea of Japan covers 978,000 km$^2$ between mainland Asia, the Korean Peninsula, the Japanese islands of Honshu and Hokkaido, and the Russian island of Sakhalin (Fig. 1a). For comparison, the total surface area of the Great Lakes is 244,000 km$^2$, with Lake Superior, the largest Great Lake, covering 82,000 km$^2$. For northwesterly flow, the maximum fetch across the Sea of Japan is ~850 km, compared to ~400 km for Lake Superior. Mean sea surface temperatures (SSTs) in the Sea of Japan generally decline westward and poleward, with warmer water where the Tsushima current flows along the west coast of Honshu and colder water where the Liman current flows along the Asian coast (Dorman et al. 2004; Lim et al. 2012; Park et al. 2014). During December, SSTs increase eastward from the Asian coast with a crescent-shaped enhanced SST gradient near the center of the Sea of Japan (Fig. 3a). SSTs decline 2°–5°C by February, with the smallest decline near the Sea of Japan coast of Russia and the largest decline near the Sea of Japan coast of north Honshu (Fig. 3b). Sea ice typically forms in the Tartary Strait in December, covers an average of 3% of the Sea of Japan at maximum extent in February, and melts by the end of March (Nihashi et al. 2017). Localized sea ice can also form along the Asian coast near and poleward of Peter the Great Gulf (Nihashi et al. 2017).

The coastal geometry and topography of the Sea of Japan region is complex and plays an important role in modulating sea-effect precipitation (Fig. 1a). To the west, the Korean Peninsula separates the Sea of Japan from the Yellow Sea and includes the Taebaek Mountains along its east coast. The Korean Highlands form a higher, broader barrier at the base of the Korean Peninsula. Lower terrain exists farther north near Peter the Great Gulf, with the Sikhote-Alin Mountains rising along the Sea of Japan coast farther northwest. Downstream of the Sea of Japan during the East Asian winter monsoon, the coastline and terrain of Honshu and Hokkaido are complex with isolated volcanic peaks and mountain barriers of various scales

and orientations. Central Honshu features the highest peaks and most sustained orography, reaching over 3,000 m MSL in the Hida Mountains, 2,400 m MSL in the Kubiki Mountains, and 2,000 m MSL in the Echigo Mountains (Fig. 1b). The terrain of northern Honshu and western Hokkaido is less formidable, but includes numerous peaks over 1,000 m, some reaching over 2,000 m (Fig. 1a). Densely populated coastal plains exist in many areas, including the Echigo Plain of central Honshu (Fig. 1b) and the Ishikari Plain surrounding Sapporo on Hokkaido (Fig. 1a).

The climate of Japan is often described as monsoonal due to the predominance of wintertime westerly to northerly flow, summertime southerly to southeasterly flow, and associated variations in precipitation (Danchenkov et al. 2000; Chang et al. 2006). This seasonal flow reversal reflects continental-scale circulation changes associated with the Asian winter and summer monsoon systems. The East Asian winter monsoon refers to the midlatitude component of the Asian winter monsoon, occurs from November to March, and features the Siberian–Mongolian high over Asia and Aleutian low over the North Pacific (Chang et al. 2006). These dominant circulation features result in frequent cold air outbreaks with westerly to northerly flow over the Sea of Japan (Yoshino 1977; Fletcher et al. 2016).

Liquid precipitation equivalent (LPE) and snowfall increase dramatically across the Sea of Japan during the East Asian winter monsoon (Fig. 4; 1981–2010 climate normals). At Vladivostok near Peter the Great Gulf, mean monthly LPE from November to March is <30 mm (1.18 in.), with a minimum of 13.4 mm (0.53 in.) in January (Tokyo Climate Center 2019). At Gangneung and Taebaek near the east coast of the Korean Peninsula, mean monthly LPE from November to March is greater, but still ≤80.3 mm (3.16 in.) (Korea Meteorological Administration 2011). Curiously, the mean monthly LPE during these months is greater at Gangneung (26 m MSL) than Teabaek (713 m MSL), despite the former's lower elevation, which likely reflects enhanced coastal precipitation associated with topographic blocking during episodic easterly flow from the Sea of Japan (e.g., Jung et al. 2012; Nam et al. 2014). The seasonal cycle at all three sites is pronounced with a maximum in July or August and a minimum in December or January. Although mean annual snowfall for these sites is unavailable and likely low, they can be affected by less frequent winter storms (e.g., Jung et al. 2012; Nam et al. 2014; Kim and Jin 2016).

In contrast, at Joetsu near the Sea of Japan coast of central Honshu, the mean monthly LPE from November to March is >190 mm and exceeds 400 mm (15.75 in.) in December and January [Fig. 4; data for all Japanese sites from Japan Meteorological Agency (2019)]. Mean annual snowfall is 635 cm (250 in.), with a peak in January. Farther inland at Tsunan in the foothills of the Echigo Mountains, the mean monthly LPE from November to March is lower than Joetsu, but still reaches over 200 mm (7.87 in.) in December and January. Mean annual snowfall is 1,349 cm (531 in.) with a monthly maximum of 443 cm (174 in.) in January, remarkable totals for a site at 452 m MSL and 37.0°N. Unlike the sites on mainland Asia, which observe their minimum monthly LPE in December or January, Joetsu and Tsunan observe their maximum LPE in those months.

Farther north at Aomori and Sapporo, monthly mean LPE from November to March is lower, but a greater fraction of precipitation falls as snow and the accumulation season is longer, leading to mean annual snowfall totals of 669 and 597 cm (263 and 235 in.), respectively, comparable to Joetsu. The seasonal cycle at these sites is limited. In the mountains above Aomori, mean annual snowfall at Sukayu Onsen (890 m MSL) is 1,764 cm (694 in.), including a peak of 459 cm (180 in.) in January.[1] Near the base of Mt. Niseko south of Sapporo, Kutchan (176 m MSL) observes a mean annual snowfall of 1,062 cm (418 in.) with a peak of 291 cm (115 in.) in January. The remarkable snowfall totals in January make this month in the mountains of Honshu and Hokkaido near the Sea of Japan the surest bet for deep-powder skiing anywhere in the world (Steenburgh 2014). Although quantifying the fraction of the LPE and snowfall produced by sea-effect processes is

[1] The Japan Meteorological Agency does not provide an official annual mean for Sukayu Onsen. The value of 1,764 cm is based on the sum of monthly means.

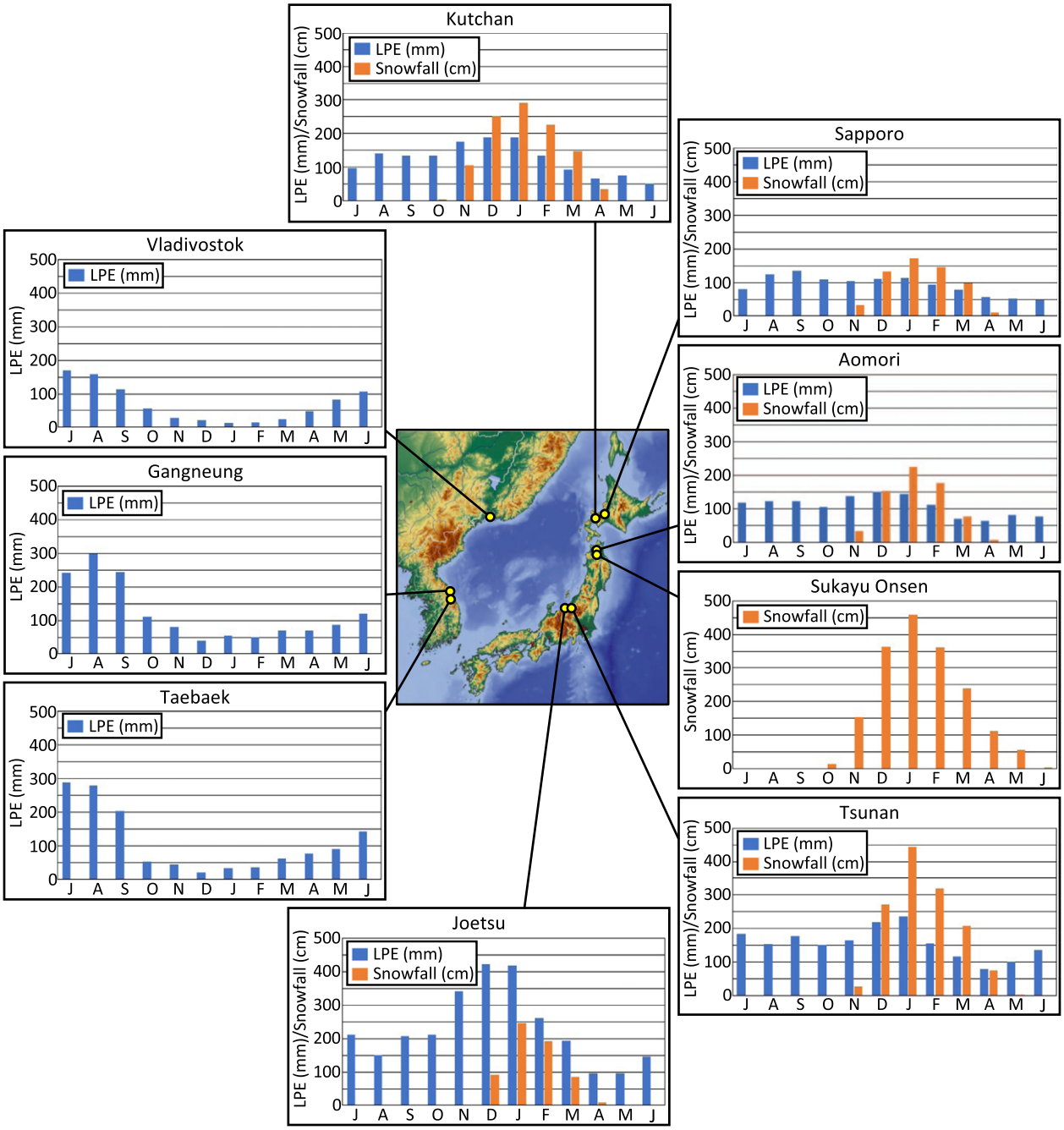


**Fig. 4. Histograms of mean monthly LPE (mm, blue bars where data available) and snowfall (cm, orange bars where data available) at selected sites in the Sea of Japan region.**

difficult, West et al. (2019) show using data from the NASA A-Train satellite constellation that clouds and precipitation produced during potential sea-effect periods compose a majority of the clouds and precipitation over the Sea of Japan and adjoining regions of Honshu and Hokkaido from December through February.

## Morphology of sea-effect systems

A wide range of cloud and precipitation patterns are produced during cold-air outbreaks over the Sea of Japan. Boundary layer circulations often lead to open-cellular convection, quasi-periodic cloud and precipitation bands oriented parallel to the mean boundary layer flow, or quasi-periodic cloud and precipitation bands oriented normal to the mean boundary layer flow (e.g., Fukatsu 1963; Tetehira and Fukatsu 1965; Tsuchiya and Fujita 1967; Miura 1986; Nakai et al. 2005; Yamada et al. 2010; Eito et al. 2010). The latter two patterns are associated

with horizontal roll convection, which produces cloud and precipitation bands that are aligned along (across) the flow during periods of weak (strong) boundary layer directional shear and are referred to in Japan as "L-mode" ("T-mode") given their longitudinal (transversal) band orientation relative to the mean boundary layer flow. The two modes can occur concurrently over the Sea of Japan due to regional variations in boundary layer depth and directional shear during cold-air outbreaks (e.g., Fig. 5).

L-mode bands are analogous to quasi-periodic wind-parallel bands found over the Laurentian Great Lakes (e.g., Kelly 1982, 1984; Kristovich 1993; Kristovich and Laird 1998), which are referred to as type-II bands by Niziol et al. (1995). T-mode bands appear to be rare over the Laurentian Great Lakes as they are not identified in climatological studies (e.g., Kristovich and Steve 1995; Veals and Steenburgh 2015; Laird et al. 2017) and we know of no case studies describing such bands in the peer-reviewed literature. The reasons for the relative scarcity of T-mode bands over the Laurentian Great Lakes are unclear.

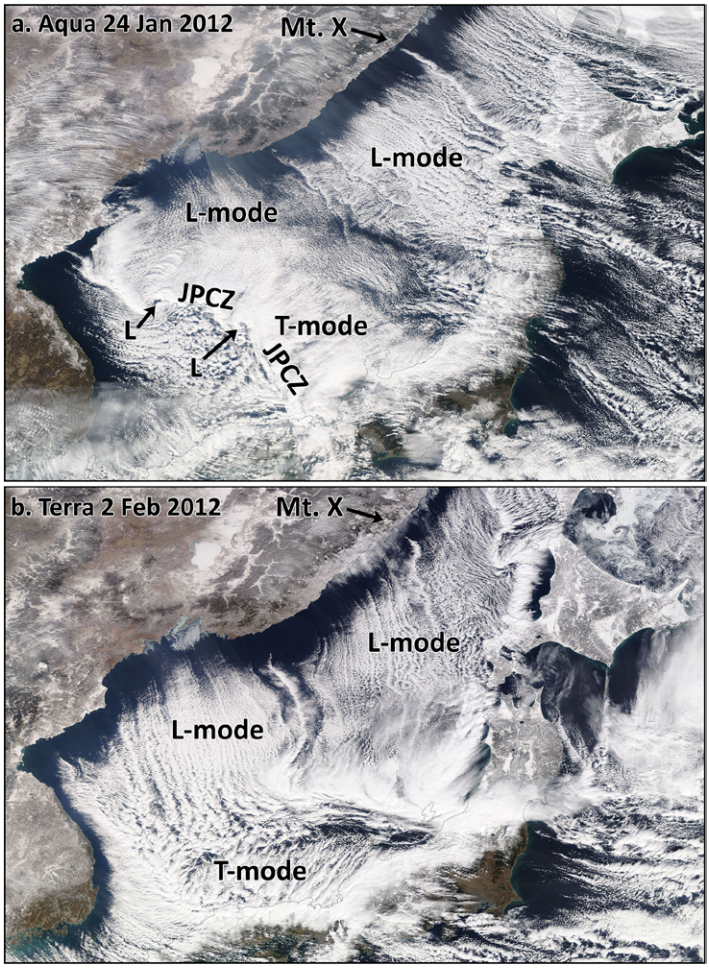


FIG. 5. NASA MODIS visible imagery of sea-effect cloud systems on (a) 24 Jan and (b) 2 Feb 2012. Morphological types defined in text; L denotes mesovortices.

In addition to boundary layer circulations, the coastal geometry and topography of mainland Asia produces circulations and low-level convergence that can generate broader, more intense cloud and precipitation bands (Fig. 5). The most prominent is the Japan Sea polar airmass convergence zone (JPCZ), which forms in response to flow interactions with the Korean Highlands and differential surface heating between the Korean Peninsula and the western Sea of Japan (Nagata et al. 1986; Nagata 1987, 1991; Asai 1988; Hozumi and Magono 1984; Eito et al. 2010; West et al. 2019). The JPCZ typically extends downstream from near the base of the Korean Peninsula, reaching the coast of Honshu between 133° and 139°E (Eito et al. 2010). There can also be a transition from L-mode to T-mode snowbands near the JPCZ (Eito et al. 2010).

Smaller-scale irregularities and topographic features along the Asian coast also modulate winds, clouds, and precipitation (Hozumi and Magono 1984; Scotti 2005). One prominent obstacle in the Sikhote-Alin Mountains, known in the literature as "Mt. X," frequently produces a cloud band that can extend to Hokkaido (Muramatsu 1979; Ohtake et al. 2009; see also Fig. 5). Occasionally, northwesterly flow from Asia converges with northeasterly flow from the Sea of Okhotsk, generating a cloud band over the northern Sea of Japan that can curve eastward into Hokkaido (Katsumata et al. 1998).

Finally, mesovortices, polar lows, and associated airmass boundaries are common over the Sea of Japan and modulate sea-effect snowfall. In some cases, the JPCZ serves as a locus for mesovortex genesis (Asai 1988; Tsuboki and Asai 2004). During one winter season, Nakai et al. (2005) identified 5 mesovortices during 46 sea-effect events affecting central Honshu. The mesovortices had diameters of 20–100 km and were often accompanied by a curved snowband and wind shift.

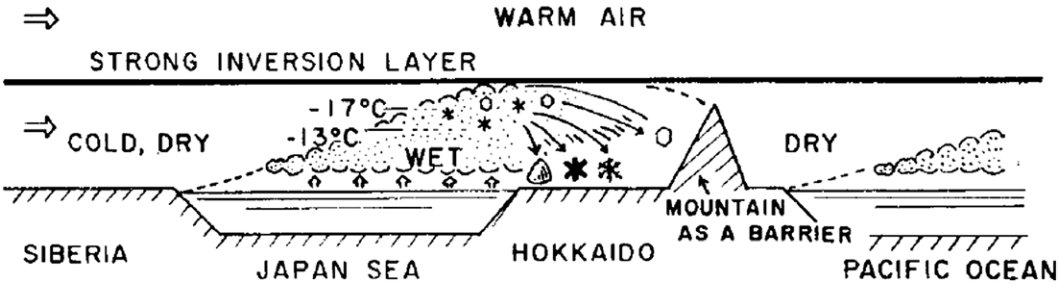


**Fig. 6. Conceptual model of satoyuki (lowland) snowfall. From Magono et al. (1966).**

## Downstream orographic effects

Formidable topography exists on Honshu and Hokkaido that strongly influences the intensity, distribution, and inland penetration of sea-effect precipitation (Veals et al. 2019). Although it is commonly assumed that precipitation and snowfall increase with altitude, events near the Sea of Japan sometimes produce heavier precipitation in the lowlands and adjoining foothills. Magono et al. (1966) distinguished between "satoyuki" snowfalls with heavier lowland accumulations and "yamayuki" snowfalls with heavier mountain accumulations, emphasizing that the former can produce damage in populated areas. They describe a conceptual model for satoyuki snowfalls that includes an inversion near mountain top and clouds confined to the windward lowlands, with heavier, rimed ice crystals such as graupel falling near the coast and lightly rimed crystals falling farther inland (Fig. 6). In some instances, katabatic flow develops along the coast, opposes the large-scale flow, and produces or enhances a land-breeze front that generates precipitation near the coast or off shore (Ishihara et al. 1989; Yoshihara et al. 2004; Eito et al. 2005). Veals et al. (2019) show that for a given flow direction (e.g., 290°), the inland penetration and orographic enhancement of sea-effect precipitation increases with the mean boundary layer (i.e., 950–800 hPa) wind speed (Fig. 7). The inland penetration of lake-effect precipitation and enhancement over the 500-m high Tug Hill Plateau similarly increases with the strength of the boundary layer flow downstream of Lake Ontario (e.g., Villani et al. 2017; Eipper et al. 2018; Veals et al. 2018).

## Microphysical processes

There is a rich history of cloud microphysical research in Japan, including the extensive observation and classification of natural snow and ice crystals based largely on samples collected near the Sea of Japan (e.g., Nakaya and Sekido 1938; Nakaya 1954; Magono and Lee 1966; Kikuchi et al. 2013). Since 2002, quasi-continuous measurements of wintertime precipitation have been made by the Falling Snow Observatory operated by the Snow and Ice Research Center at the National Research Institute for Earth Science and Disaster Resilience in Nagaoka near the Sea of Japan coast of central Honshu (Ishizaka et al. 2013; see Fig. 1b for location). The typical surface temperature in Nagaoka during winter precipitation is ~0°C (Yamaguchi et al. 2013), which leads to the frequent generation of snow aggregates composed of well-rimed dendrites that can exceed a size of 10 mm (Ishizaka et al. 2013). Graupel is also common due to the strong updrafts and large supercooled cloud water concentrations in sea-effect clouds, which leads to accretional growth (Murakami et al. 1994). L-mode snowbands in particular often bring snowfall composed mostly of graupel, which has spherical or conical shapes and forms a layer within the snowpack with a small particle-to-particle contact area. Such a layer tends to be weak (i.e., less cohesive) and can serve as the failure layer for avalanches (Abe 2004). "Graupel" here not only refers to particles with diameters up to 5 mm, but also spherical and conical soft hail with a diameter of 7 mm, which is common in Nagaoka. Sometimes the diameter exceeds even 10 mm. Such particles are soft and easily crushed when squeezed between two fingers, indicating that the particle does not experience the wet-growth process.

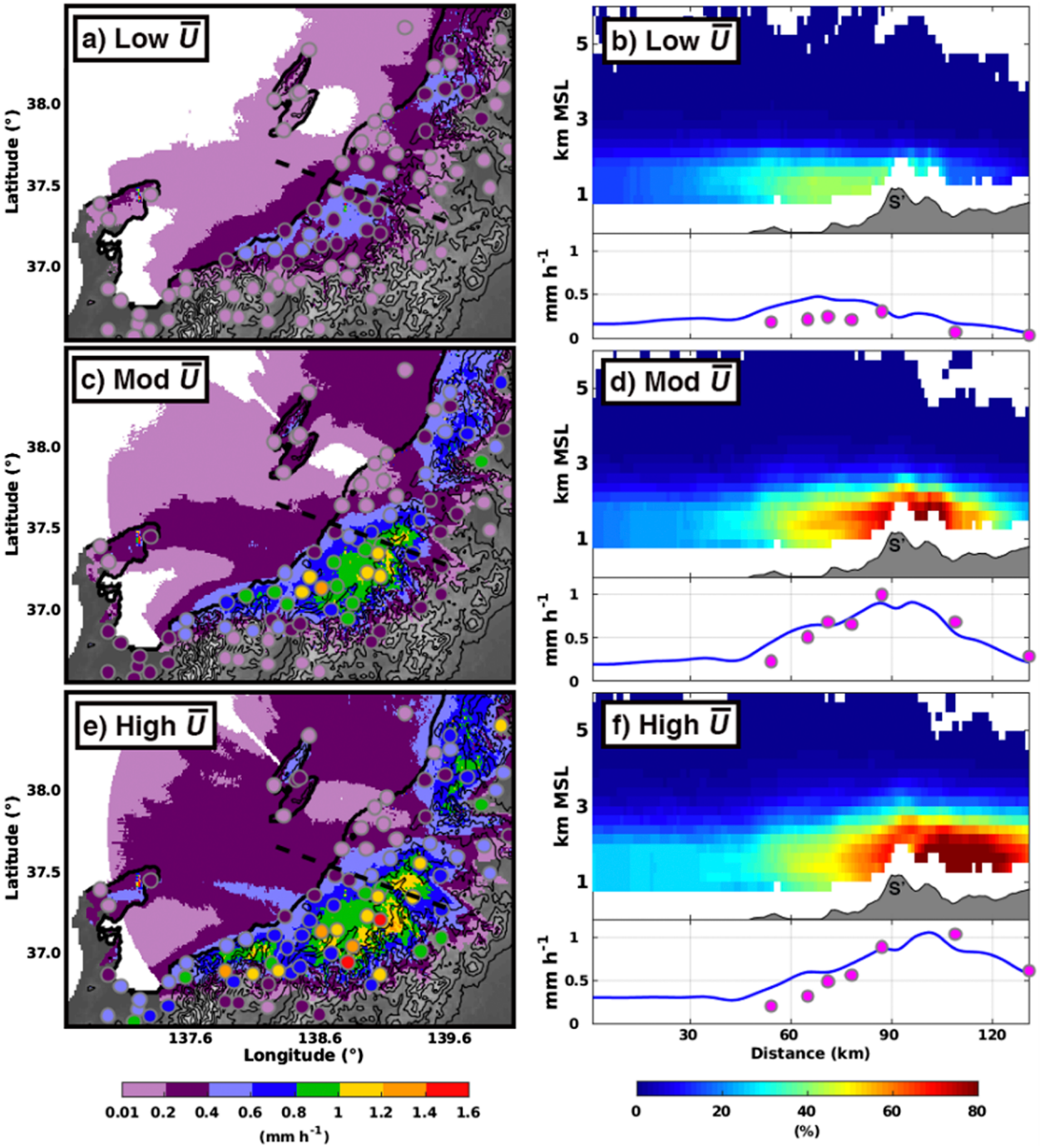


**Fig. 7. (a) Mean radar-derived (color shading) and gauge (filled circles) LPE rate (mm h$^{-1}$ following scale at bottom left) during sea-effect periods with a mean 950–800 hPa wind direction of 290° and wind speed ≤8.8 m s$^{-1}$. (b) Frequency of radar echoes >10 dB*Z* (color shading following scale at bottom right), terrain (gray shaded), mean radar-derived LPE rate (blue line), and gauge LPE rate (circles) along transect denoted by dashed line in (a). (c),(d) and (e),(f) As in (a),(b), but for mean wind speeds of 11.5–13.6 m s$^{-1}$ and ≥16.4 m s$^{-1}$, respectively. From Veals et al. (2019).**

Kajikawa (1976) showed that the density of graupel particles in sea-effect storms varies significantly, which may cause large uncertainty in the calculation of radar backscattering and quantitative precipitation estimates from radar.

Graupel falls predominantly in coastal areas, producing as much as one-third of the precipitation during January along the Sea of Japan coast of central Honshu (Mizuno 1992). A decline in graupel farther inland may reflect the loss of surface sensible and latent heating and the resulting decline in updraft strength, supercooled liquid water availability, and accretional growth (Takeda et al. 1982; Harimaya and Kanemura 1995). The causes of this inland

transition have not been carefully investigated, but such changes are broadly consistent with the convective-to-stratiform transition that occurs, for example, downstream of Lake Ontario (Minder et al. 2015). Nevertheless, in some instances orographic updrafts generated by Japanese topography can counter this transition and increase supercooled liquid water availability, accretional growth, and graupel production or size (Nakai et al. 1998).

Mesoscale snowbands generated by the JPCZ can produce heavy snowfall and typically reach greater heights than other sea-effect systems. Murakami (2019) presents a conceptual model of JPCZ cloud bands based on aircraft and ship observations that features a cloud top that reaches nearly 6 km, suggesting significant ice nucleation in the low temperature environment. Aircraft observations have revealed high ice crystal concentrations reaching 1,000 $L^{-1}$ and 0.3 g $m^{-3}$ in the well-developed convective cloud region of JPCZ (Murakami 2019).

## Hazards and benefits

The combination of extreme snowfall and high population density near the Sea of Japan poses great challenges for public safety, road and sidewalk maintenance, and avalanche mitigation. Although estimates vary, Japan likely averages over 100 deaths and 400 injuries each year due to snow and ice hazards, with most victims succumbing due to snow-removal activities (Nakai et al. 2012; Heimburger 2018, p. 32). Structural collapses, "roofalanches" (masses of snow sliding off of roofs), and avalanches also cause fatalities. The 1963 "gosetsu" (heavy snowfall) winter led to 231 fatalities and 1,735 total or partially damaged homes nationwide (Nakamura and Shimizu 1996; Heimburger 2018). Snow depths reached 3.18 m in Nagaoka (21 m MSL). The 1918 Mitsumata avalanche disaster in the Niigata prefecture, which killed 155, ranks as the one of the 10 worst avalanche disasters by deaths worldwide since the sixteenth century (Ancey 2016). North of Hokkaido, Russia's Sakhalin Island east of the Sea of Japan and Kuril Islands east of the Sea of Okhotsk also see frequent sea-effect snowfalls and, while the population density is low, their per capita avalanche fatality rate is among the highest in the world (Podolskiy et al. 2019). Most of the victims are residents and workers, rather than recreationists.

Coastal cities of central Honshu near the Sea of Japan experience relatively mild winters with mean surface temperatures >0°C even during the months of January and February (Ishizaka 2004; Kawase et al. 2013). With temperatures frequently near or even above the melting point, groundwater spraying onto roadways or sidewalks is used extensively to melt and remove snow (Fig. 8). In Obama City, for example, the mean annual snowfall is 179 cm (70 in.), but the daily mean temperature in January, the coldest month of the year, is 3.7°C. Groundwater used for snowmelt accounted for 13% of the groundwater usage in Obama City in 2011 (the remaining use was primarily domestic, including drinking water), but its use for snow removal offered a substantial


FIG. 8. Snow melting and removal using (a) road sprinklers in Nagano and (b) water tubes at the Snow and Ice Research Center in Nagaoka.

savings over conventional approaches (Burnett et al. 2018). Elsewhere, road and sidewalk heating systems are deployed in many areas and snow-flowing roadside gutter systems and snow-melting tanks are used in Sapporo to melt and remove snow (Morita and Tago 2005; Permanent International Association of Road Congresses 2014). During fiscal year 2018, Sapporo plowed or removed snow from 5,711 km of roads and 3,033 km of sidewalks, operated road heating systems at 547 locations, and utilized 8 snow-flowing gutters and 11 snow-melting tanks (City of Sapporo 2019). The gutters drain downslope and contain free-flowing river water or warm treated sewage effluent that melts snow that is dumped through grates by residents. The tanks are used to dispose snow removed from roads, with sewage effluent or heating from waste incineration providing energy for snowmelt (Permanent International Association of Road Congresses 2014).

Japan has extensive road weather information systems and the Snow and Ice Research Center at the National Research Institute for Earth Science and Disaster Resilience has developed a Snow Disaster Forecasting System (SDFS) for predicting avalanche potential, reduced visibility, road conditions, and snow accretion (Nakai et al. 2012; Permanent International Association of Road Congresses 2014; Nakai et al. 2019). The SDFS integrates atmospheric (large scale and cloud resolving), snow metamorphism, blowing snow, avalanche, and road-weather models.

Skiers, snowboarders, and Japan's winter-sports economy are major beneficiaries of this snowfall. Sapporo and Nagano each hosted an Olympic Winter Games in 1972 and 1998, respectively, and there are over 500 ski and snowboard areas in Japan.

## Vulnerability to climate change

In mild coastal regions along the Sea of Japan, diabatic cooling produced by melting and sublimating snow is often critical for lowering snow levels and produces a pronounced peak in precipitation frequency at surface (i.e., 2 m) temperatures near 0°C [e.g., Nagaoka (Fig. 9); Yamaguchi et al. 2013]. This yields great sensitivity of precipitation type (rain or snow) to temperature, with snowfall fraction, snow depth, and snow-cover duration declining abruptly with a small increase in temperature (Suzuki 2006; Yamaguchi et al. 2011; Kawase et al. 2012). Ishii and Suzuki (2011) document significant long-term declines in snowfall in these temperature-sensitive coastal regions from 1962 to 2009. More recently the Japan Meteorological Agency reported that from 1962 to 2017 the ratio of annual maximum snow depth relative to the 1981–2010 average declined at low-elevation sites near the Sea of Japan at a rate of 13.8% per decade in western Honshu (95% confidence level), 12.3% per decade in central Honshu (99% confidence level), and 3.3% per decade (90% confidence level) in northern Honshu and Hokkaido (Japan Meteorological Agency 2018).

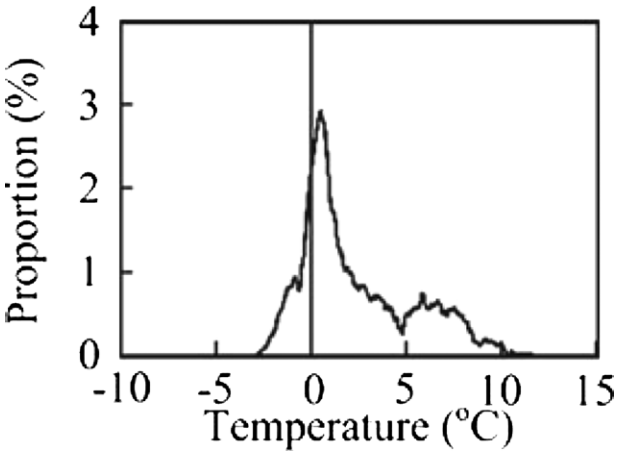


**Fig. 9. Proportion of the winter (December–February) LPE vs surface (i.e., 2 m) temperature at Nagaoka. Adapted from Yamaguchi et al. (2013).**

At higher elevations, however, Ishii and Suzuki (2011) did not find significant long-term trends in snowfall and Yamaguchi et al. (2011) found no notable increases in mean winter temperature or reduction in maximum snow depth and maximum snowpack water equivalent at recently installed mountain observing sites in central Honshu from 1990 to 2010, although they note this is a short data record. It appears that declines in snowfall and snowpack associated with long-term warming trends are most evident in relatively warm, low-latitude and low-elevation regions near the Sea of Japan, but to date are weak or undetectable in relatively cold, high-latitude or high-elevation regions. Snow measures exhibit similar temperature

and altitudinal dependencies in western North America (e.g., Pierce et al. 2008; Pierce and Cayan 2013).

Regional climate modeling studies suggest, however, that declines in snowfall and snowpack will eventually occur at all elevations. For example, pseudo-global-warming ensembles for central Honshu near the Sea of Japan that assume ~2°C of regional wintertime warming feature reduced maximum snow depths at all elevations, with declines of 20%–54% near sea level and 8%–22% above 2,000 m depending on the experiment (Kawase et al. 2013, see their Fig. 4). Snowfall similarly declines 35%–47% near sea level and 0%–12% above 2,000 m (Kawase et al. 2013, see their Fig. 6). The experiment with no snowfall decline above 2,000 m featured a 6% increase in precipitation, which offsets declines in the fraction of precipitation falling as snow. However, regional climate model ensembles based on accelerated [i.e., representative concentration pathway 8.5 (RCP8.5)] scenarios suggest a decline in winter (December–February) precipitation along all of Honshu and southwest Hokkaido near the Sea of Japan due to a weaker winter monsoon (Kawase et al. 2015, 2016). In contrast, precipitation increases over northwest and interior Hokkaido due to stronger northwesterly flow over the northern Sea of Japan in response to decreased ice cover over the Sea of Okhotsk, as well as an increase of high-latitude humidity (Kawase et al. 2015). Nevertheless, total winter snowfall declines along all of Honshu and Hokkaido near the Sea of Japan except in the highest, interior region of Hokkaido (Fig. 10). These results suggest long-term declines in snowfall and snowpack are likely across most of Japan's gosetsu chitai during the twenty-first century, with the declines largest in lower-latitude regions near sea level and smallest at higher altitudes and latitudes. Paradoxically, regional climate simulations under an RCP8.5 scenario suggest an increase in the magnitude of the most extreme daily snowfall events in areas just inland from the Sea of Japan (Kawase et al. 2016). These areas remain cold enough to observe larger daily snowfall totals produced by more intense mesoscale convergence along the JPCZ or orographic effects even as snowpack and total snowfall decline.

## Summary

Frequent sea-effect precipitation produces prolific snowfalls and deep seasonal snowpacks during the East Asian winter monsoon in Japan's "gosetsu chitai" (heavy snow region) near the Sea of Japan. Extensive research describes the structure, dynamics, and microphysical processes of sea-effect precipitation systems, public safety and snow removal activities, and recent and projected long-term trends in snowfall and snowpack in this region. Compared with similar storms produced by the Laurentian Great Lakes, sea-effect systems generated by the Sea of Japan are modulated by the regional coastal geometry and topography, extend to greater depth, and more frequently feature transversal-mode snowbands. Significant infrastructure exists for snow removal, which, in some regions, uses techniques (e.g.,

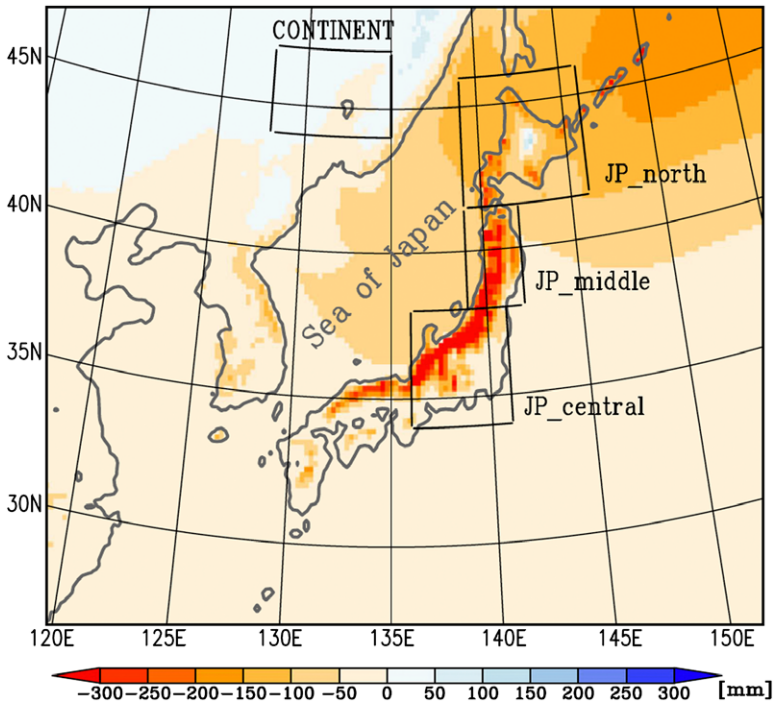


**Fig. 10. Projected change in total winter monsoon (November–March) snowfall (LPE) based on a historical climate ensemble (1950–2011) and a future climate ensemble based on a global mean temperature that is 4°C warmer than the preindustrial climate. From Kawase et al. (2016).**

groundwater spraying) that are not widely deployed in North America but take advantage of the relatively mild, coastal snow climate. Snowfall and snowpacks in coastal areas of western and central Honshu near the Sea of Japan are especially vulnerable to global warming, although snowfall and snowpack are projected to decline even in colder higher-latitude and higher-altitude regions of Japan under high emissions scenarios.

There is significant potential to advance our understanding and prediction of sea- and lake-effect precipitation through increased awareness of research from the Sea of Japan region and strengthening collaborations between scientists in North America, Japan, East Asia, and other sea- and lake-effect regions. In particular, comparison of the characteristics of sea- and lake-effect systems in various regions of the world is important for understanding the fundamental processes that control the mode of sea- and lake-effect systems and their influence on the intensity and distribution of precipitation. Clarifying the regional microphysical differences of sea- and lake-effect clouds may lead to the improvement of quantitative precipitation estimates from meteorological radars and the parameterization of microphysical processes by numerical models.

**Acknowledgments.** This article is based in part on collaborative research supported by the U.S. National Science Foundation under Grant AGS-1635654. Any opinions, findings, and conclusions or recommendations expressed in this material are those of the authors and do not necessarily reflect the views of the National Science Foundation. This article would not have been possible without insights and contributions from Peter Veals, Leah Campbell, Tom Gowan, and Tyler West at the University of Utah and Ryohei Misumi and Kazuki Nakamura at the National Research Institute for Earth Science and Disaster Resilience. Comments from Scott Steiger and two anonymous reviewers improved the manuscript.

## References


Abe, O., 2004: Shear strength and angle of repose of snow layers including graupel. *Ann. Glaciol.*, **38**, 305–308, https://doi.org/10.3189/172756404781815149.

Ancey, C., 2016: Snow avalanches. *Natural Hazard Science*, *Oxford Research Encyclopedia*, Oxford University Press, https://doi.org/10.1093/acrefore/9780199389407.013.17.

Asai, T., 1988: Meso-scale features of heavy snowfalls in Japan Sea coastal regions of Japan (in Japanese). *Tenki*, **35**, 156–161.

Bao, B., and G. Ren, 2018: Sea-effect precipitation over the Shandong Peninsula, northern China. *J. Appl. Meteor. Climatol.*, **57**, 1291–1308, https://doi.org/10.1175/JAMC-D-17-0200.1.

Burnett, K. M., C. A. Wada, M. Taniguchi, R. Sugimoto, and D. Tahara, 2018: Evaluating the tradeoffs between groundwater pumping for snow-melting and nearshore fishery productivity in Obama City, Japan. *Water*, **10**, 1556, https://doi.org/10.3390/w10111556.

Byrd, G. P., R. A. Anstett, J. E. Heim, and D. M. Usinski, 1991: Mobile sounding observations of lake-effect snow bands in western and central New York. *Mon. Wea. Rev.*, **119**, 2323–2332, https://doi.org/10.1175/1520-0493(1991)119<2323:MSOOLE>2.0.CO;2.

Chang, C.-P., Z. Wang, and H. Hendon, 2006: The Asian winter monsoon. *The Asian Monsoon*, B. Wang, Ed., Springer, 89–127.

City of Sapporo, 2019: Sapporo 2019: Facts and figures. City of Sapporo Rep., 6 pp., www.city.sapporo.jp/kokusai/documents/sapporo2019factsfigure.pdf.

Danchenkov, M. A., D. G. Aubrey, and G. H. Hong, 2000: Bibliography of the oceanography of the Japan/East Sea. North Pacific Marine Science Organization Scientific Rep. 13, 99 pp.

Dorman, C. E., R. C. Beardsley, N. A. Dashko, C. A. Friehe, D. Kheilf, K. Cho, R. Limeburner, and S. M. Varlamov, 2004: Winter marine atmospheric conditions over the Japan Sea. *J. Geophys. Res.*, **109**, C12011, https://doi.org/10.1029/2001JC001197.

Eipper, D. T., G. S. Young, S. J. Greybush, S. Saslo, T. D. Sikora, and R. D. Clark, 2018: Predicting the inland penetration of long-lake-axis-parallel snowbands. *Wea. Forecasting*, **33**, 1435–1451, https://doi.org/10.1175/WAF-D-18-0033.1.

Eito, H., T. Kato, M. Yoshizaki, and A. Adachi, 2005: Numerical simulation of the quasi-stationary snowband observed over the southern coastal area of the Sea of Japan on 16 January 2001. *J. Meteor. Soc. Japan*, **83**, 551–576, https://doi.org/10.2151/jmsj.83.551.

——, M. Murakami, C. Muroi, T. Kato, S. Hayashi, H. Kuroiwa, and M. Yoshizaki, 2010: The structure and formation mechanism of transversal cloud bands associated with the Japan-sea polar-airmass convergence zone. *J. Meteor. Soc. Japan*, **88**, 625–648, https://doi.org/10.2151/jmsj.2010-402.

Fletcher, J., S. Mason, and C. Jakob, 2016: The climatology, meteorology, and boundary layer structure of marine cold air outbreaks in both hemispheres. *J. Climate*, **29**, 1999–2014, https://doi.org/10.1175/JCLI-D-15-0268.1.

Fukatsu, H., 1963: On the snow shower in Tokai and Hokuriku Districts as seen by radar echoes (in Japanese). *Tenki*, **10**, 373–377.

Harimaya, T., and N. Kanemura, 1995: Comparison of the riming growth of snow particles between coastal and inland areas. *J. Meteor. Soc. Japan*, **73**, 25–36, https://doi.org/10.2151/jmsj1965.73.1_25.

Heimburger, J.-F., 2018: *Japan and Natural Disasters: Prevention and Risk Management.* John Wiley and Sons, 228 pp.

Hozumi, K., and C. Magono, 1984: The cloud structure of convergent cloud bands over the Japan Sea in winter monsoon period. *J. Meteor. Soc. Japan*, **62**, 522–533, https://doi.org/10.2151/jmsj1965.62.3_522.

Ishihara, M., H. Sakakibara, and Z. Yanagisawa, 1989: Doppler radar analysis of the structure of mesoscale snow bands developed between the winter monsoon and the land breeze. *J. Meteor. Soc. Japan*, **67**, 503–520, https://doi.org/10.2151/jmsj1965.67.4_503.

Ishii, H., and K. Suzuki, 2011: Regional characteristics of variation of snowfall in Japan. *J. Japan Hydrol. Sci.*, **41**, 27–37, https://doi.org/10.4145/jahs.41.27.

Ishizaka, M., 2004: Climatic response of snow depth to recent warmer winter seasons in heavy-snowfall areas in Japan. *Ann. Glaciol.*, **38**, 299–304, https://doi.org/10.3189/172756404781815248.

——, H. Motoyoshi, S. Nakai, T. Shiina, T. Kumakura, and K. Muramoto, 2013: A new method for identifying the main type of solid hydrometeors contributing to snowfall from measured size-fall speed relationship. *J. Meteor. Soc. Japan*, **91**, 747–762, https://doi.org/10.2151/jmsj.2013-602.

Japan Meteorological Agency, 2018: Climate monitoring report 2017. Japan Meteorological Agency Rep., 93 pp., www.jma.go.jp/jma/en/NMHS/ccmr/ccmr2017_high.pdf.

——, 2019: Past weather data search. Japan Meteorological Agency, accessed 9 July 2019, www.data.jma.go.jp/obd/stats/etrn/index.php.

Jung, S.-H., E.-S. Im, and S.-O. Han, 2012: The effect of topography and sea surface temperature on heavy snowfall in the Yeongdong region: A case study with high resolution WRF simulation. *Asia-Pac. J. Atmos. Sci.*, **48**, 259–273, https://doi.org/10.1007/s13143-012-0026-2.

Kajikawa, M., 1976: Observation of density of graupel particles (in Japanese). *Tenki*, **23**, 685–695.

Katsumata, M., H. Uyeda, and K. Kikuchi, 1998: Characteristics of a cloud band off the west coast of Hokkaido Island as determined from AVHRR/NOAA, SSM/I and radar data. *J. Meteor. Soc. Japan*, **76**, 169–189, https://doi.org/10.2151/jmsj1965.76.2_169.

Kawase, H., and Coauthors, 2012: Downscaling of snow cover changes in the late 20th century using a past climate simulation method over central Japan. *SOLA*, **8**, 61–64, https://doi.org/10.2151/sola.2012-016.

——, and Coauthors, 2013: Altitude dependency of future snow cover changes over central Japan evaluated by a regional climate model. *J. Geophys. Res. Atmos.*, **118**, 12 444–12 457, https://doi.org/10.1002/2013JD020429.

——, H. Sasaki, A. Murata, M. Nosaka, and N. N. Ishizaki, 2015: Future changes in winter precipitation around Japan projected by ensemble experiments using NHRCM. *J. Meteor. Soc. Japan*, **93**, 571–580, https://doi.org/10.2151/jmsj.2015-034.

——, and Coauthors, 2016: Enhancement of heavy daily snowfall in central Japan due to global warming as projected by large ensemble of regional climate simulations. *Climatic Change*, **139**, 265–278, https://doi.org/10.1007/s10584-016-1781-3.

Kelly, R. D., 1982: A single Doppler radar study of horizontal-roll convection in a lake-effect snow storm. *J. Atmos. Sci.*, **39**, 1521–1531, https://doi.org/10.1175/1520-0469(1982)039<1521:ASDRSO>2.0.CO;2.

——, 1984: Horizontal roll and boundary-layer interrelationships observed over Lake Michigan. *J. Atmos. Sci.*, **41**, 1816–1826, https://doi.org/10.1175/1520-0469(1984)041<1816:HRABLI>2.0.CO;2.

Kikuchi, K., and Coauthors, 2013: A global classification of snow crystals, ice crystals, and solid precipitation based on observations from middle latitudes to polar regions. *Atmos. Res.*, **132–133**, 460–472, https://doi.org/10.1016/j.atmosres.2013.06.006.

Kim, T., and E. K. Jin, 2016: Impact of an interactive ocean on numerical weather prediction: A case of a local heavy snowfall event in eastern Korea. *J. Geophys. Res. Atmos.*, **121**, 8243–8253, https://doi.org/10.1002/2016JD024763.

Korea Meteorological Administration, 2011: Climatological normals of Korea. Korea Meteorological Administration Publ. 11-1360000-000077-14, 688 pp., www.kma.go.kr/down/Climatological_2010.pdf.

Kristovich, D. A. R., 1993: Mean circulations of boundary-layer rolls in lake-effect snow storms. *Bound.-Layer Meteor.*, **63**, 293–315, https://doi.org/10.1007/BF00710463.

——, and R. A. Steve III, 1995: A satellite study of cloud-band frequencies over the Great Lakes. *J. Appl. Meteor.*, **34**, 2083–2090, https://doi.org/10.1175/1520-0450(1995)034<2083:ASSOCB>2.0.CO;2.

——, and N. F. Laird, 1998: Observations of widespread lake-effect cloudiness: Influences of lake surface temperature and upwind conditions. *Wea. Forecasting*, **13**, 811–821, https://doi.org/10.1175/1520-0434(1998)013<0811:OOWLEC>2.0.CO;2.

Laird, N. F., N. D. Metz, L. Gaudet, C. Grasmick, L. Higgins, C. Loeser, and D. A. Zelinsky, 2017: Climatology of cold season lake-effect cloud bands for the

North American Great Lakes. *Int. J. Climatol.*, **37**, 2111–2121, https://doi.org/10.1002/joc.4838.

Lim, S., C. J. Jang, I. S. Oh, and J. Park, 2012: Climatology of the mixed layer depth in the East/Japan Sea. *J. Mar. Syst.*, **96–97**, 1–14, https://doi.org/10.1016/j.jmarsys.2012.01.003.

Magono, C., and C. W. Lee, 1966: Meteorological classification of natural snow crystals. *J. Fac. Sci. Hokkaido Univ. Ser. 7*, **2**, 321–335.

——, K. Kikuchi, T. Kimura, S. Tazawa, and T. Kasai, 1966: A study on the snowfall in the winter monsoon season in Hokkaido with special reference to low land snowfall. *J. Fac. Sci. Hokkaido Univ. Ser. 7*, **2**, 287–308.

Manabe, S., 1957: On the modification of air-mass over the Japan Sea when the outburst of cold air predominates. *J. Meteor. Soc. Japan*, **35**, 311–326, https://doi.org/10.2151/jmsj1923.35.6_311.

Melin, F., 2013: GMIS—PATHFINDER monthly climatology sea surface temperature (9km) in degree-C. European Commission Joint Research Centre, accessed 26 April 2019, http://data.europa.eu/89h/843f10d3-ecee-483e-b359-ef1ba679fb83.

Minder, J. R., T. Letcher, L. S. Campbell, P. G. Veals, and W. J. Steenburgh, 2015: The evolution of lake-effect convection during landfall and orographic uplift as observed by profiling radars. *Mon. Wea. Rev.*, **143**, 4422–4442, https://doi.org/10.1175/MWR-D-15-0117.1.

Miura, Y., 1986: Aspect ratios of longitudinal rolls and convection cells observed during cold air outbreaks. *J. Atmos. Sci.*, **43**, 26–39, https://doi.org/10.1175/1520-0469(1986)043<0026:AROLRA>2.0.CO;2.

Mizuno, H., 1992: Statistical characteristics of graupel precipitation over the Japan Island. *J. Meteor. Soc. Japan*, **70**, 115–121, https://doi.org/10.2151/jmsj1965.70.1_115.

Morita, K., and M. Tago, 2005: Snow-melting on sidewalks with ground-coupled heat pumps in a heavy snowfall city. *Proc. World Geothermal Congress*, Antalya, Turkey, International Geothermal Association, www.geothermal-energy.org/pdf/IGAstandard/WGC/2005/1443.pdf.

Murakami, M., 2019: Inner structures of snow clouds over the Sea of Japan observed by instrumented aircraft: A review. *J. Meteor. Soc. Japan*, **97**, 5–38, https://doi.org/10.2151/jmsj.2019-009.

——, M., T. Matsuo, H. Mizuno, and Y. Yamada, 1994: Mesoscale and microscale structures of snow clouds over the Sea of Japan. Part I: Evolution of microphysical structures in short-lived convective snow clouds. *J. Meteor. Soc. Japan*, **72**, 671–694, https://doi.org/10.2151/jmsj1965.72.5_671.

——, and Coauthors, 2003: The precipitation process in convective cells embedded in deep snow bands over the Sea of Japan. *J. Meteor. Soc. Japan*, **81**, 515–531, https://doi.org/10.2151/jmsj.81.515.

Muramatsu, T., 1979: The cloud line enhanced by upwind orographic features in winter monsoon situations. *Geophys. Mag.*, **38**, 1–15.

Nagata, M., 1987: On the formation of a convergent cloud band over the Japan Sea in winter; a prediction experiment. *J. Meteor. Soc. Japan*, **65**, 871–883, https://doi.org/10.2151/jmsj1965.65.6_871.

——, 1991: Further numerical study on the formation of the convergent cloud band over the Japan Sea in winter. *J. Meteor. Soc. Japan*, **69**, 419–428, https://doi.org/10.2151/jmsj1965.69.3_419.

——, M. Ikawa, S. Yoshizumi, and T. Yoshida, 1986: On the formation of a convergent cloud band over the Japan Sea in winter; numerical experiments. *J. Meteor. Soc. Japan*, **64**, 841–855, https://doi.org/10.2151/jmsj1965.64.6_841.

Nakai, S., M. Maki, and T. Yagi, 1990: Doppler radar observation of orographic modification of snow clouds—A case of enhanced snowfall. National Research Institute for Earth Science and Disaster Prevention Rep. 45, 16 pp.

——, M. Kajikawa, and Y. Yamada, 1998: The relation between prevailing precipitation-particle type and radar echo structure around the Dewa Hills. *Atmos. Res.*, **47–48**, 97–112, https://doi.org/10.1016/S0169-8095(98)00053-2.

——, K. Iwanami, R. Misumi, S. Park, M. Shimizu, and T. Kobayashi, 2003: Relation between snow-cloud mode and snowfall distribution observed in central Niigata prefecture. National Research Institute for Earth Science and Disaster Prevention Rep. 64, 8 pp.

——, ——, ——, S.-G. Park, and T. Kobayashi, 2005: A classification of snow clouds by Doppler radar observations at Nagaoka, Japan. *SOLA*, **1**, 161–164, https://doi.org/10.2151/sola.2005-042.

——, and Coauthors, 2012: A Snow Disaster Forecasting System (SDFS) constructed from field observations and laboratory experiments. *Cold Reg. Sci. Technol.*, **70**, 53–61, https://doi.org/10.1016/j.coldregions.2011.09.002.

——, and Coauthors, 2019: Study on advanced snow information and its application to disaster mitigation: An overview. *Bull. Glaciol. Res.*, **37**, 3–19, https://doi.org/10.5331/bgr.18sw01.

Nakamura, T., and M. Shimizu, 1996: Variation of snow, winter precipitation and winter air temperature during the last century at Nagaoka, Japan. *J. Glaciol.*, **42**, 136–140, https://doi.org/10.1017/S0022143000030598.

Nakaya, U., 1954: *Snow Crystals: Natural and Artificial.* Harvard University Press, 510 pp.

——, and Y. Sekido, 1938: General classification of snow crystals and their frequency of occurrence. *Bull. Hokkaido Teikoku University*, **1**, 234–264.

Nam, H., B. G. Kim, S. O. Han, C. Lee, and S. S. Lee, 2014: Characteristics of easterly-induced snowfall in Yeongdong and its relationship to air-sea temperature difference. *Asia-Pac. J. Atmos. Sci.*, **50**, 541–552, https://doi.org/10.1007/s13143-014-0044-3.

Nihashi, S., K. I. Ohshima, and S.-I. Saitoh, 2017: Sea-ice production in the northern Japan Sea. *Deep-Sea Res. I*, **127**, 65–76, https://doi.org/10.1016/j.dsr.2017.08.003.

Niziol, T. A., W. R. Snyder, and J. S. Waldstreicher, 1995: Winter weather forecasting throughout the eastern United States. Part IV: Lake effect snow. *Wea. Forecasting*, **10**, 61–77, https://doi.org/10.1175/1520-0434(1995)010<0061:WWFTTE>2.0.CO;2.

Ohigashi, T., and K. Tsuboki, 2007: Shift and intensification processes of the Japan-Sea polar-airmass convergence zone associated with the passage of a mid-tropospheric cold core. *J. Meteor. Soc. Japan*, **85**, 633–662, https://doi.org/10.2151/jmsj.85.633.

——, ——, Y. Schusse, and H. Uyeda, 2014: An intensification process of a winter broad cloud band on a flank of the mountain region along the Japan-Sea coast. *J. Meteor. Soc. Japan*, **92**, 71–93, https://doi.org/10.2151/jmsj.2014-105.

Ohtake, H., M. Kawashima, and Y. Fujiyoshi, 2009: The formation mechanism of a thick cloud band over the northern part of the Sea of Japan during cold air outbreaks. *J. Meteor. Soc. Japan*, **87**, 289–306, https://doi.org/10.2151/jmsj.87.289.

Park, K.-A., E.-Y. Lee, X. Li, S.-R. Chung, E.-H. Sohn, and S. Hong, 2014: NOAA/AVHRR sea surface temperature accuracy in the East/Japan Sea. *Int. J. Digital Earth*, **8**, 784–804, https://doi.org/10.1080/17538947.2014.937363.

Permanent International Association of Road Congresses, 2014: Snow and ice databook 2014. Permanent International Association of Road Congresses Rep., 223 pp., www.piarc.org/en/order-library/22913-en-Snow%20and%20Ice%20Databook%202014.htm.

Pierce, D. W., and D. R. Cayan, 2013: The uneven response of different snow measures to human-induced climate warming. *J. Climate*, **26**, 4148–4167, https://doi.org/10.1175/JCLI-D-12-00534.1.

——, and Coauthors, 2008: Attribution of declining western U.S. snowpack to human effects. *J. Climate*, **21**, 6425–6444, https://doi.org/10.1175/2008JCLI2405.1.

Podolskiy, E. A., K. Izumi, V. E. Suchkov, and N. Eckert, 2014: Physical and societal statistics for a century of snow-avalanche hazards on Sakhalin and the Kuril Islands (1910–2010). *J. Glaciol.*, **60**, 409–430, https://doi.org/10.3189/2014JoG13J143.

Scotti, A. D., 2005: Orographic effects during winter cold-air outbreaks over the Sea of Japan (East Sea): Results from a shallow-layer model. *Deep-Sea Res. II*, **52**, 1705–1725, https://doi.org/10.1016/j.dsr2.2004.06.038.

Steenburgh, J., 2014: *Secrets of the Greatest Snow on Earth.* Utah State University Press, 186 pp.

Suzuki, H., 2006: Long-term changes in snowfall depth and snow cover depth in and around Niigata prefecture from 1927 to 2005: Analysis using data observed at railway stations (in Japanese). *Tenki*, **53**, 185–196.

Takeda, T., and Coauthors, 1982: Modification of convective snow-clouds in landing the Japan Sea coastal region. *J. Meteor. Soc. Japan*, **60**, 967–977, https://doi.org/10.2151/jmsj1965.60.4_967.

Tetehira, R., and H. Fukatsu, 1965: Radar analyses of Hokuriku heavy snowfall (in Japanese). *Tenki*, **12**, 319–322.

Tokyo Climate Center, 2019: Normals data Vladivostok: Russian Federation (In Asia). Japan Meteorological Agency, accessed 9 July 2019, https://ds.data.jma.go.jp/tcc/tcc/products/climate/normal/parts/NrmMonth_e.php?stn=31960.

Tsuboki, K., and T. Asai, 2004: The multi-scale structure and development mechanism of mesoscale cyclones over the Sea of Japan in winter. *J. Meteor. Soc. Japan*, **82**, 597–621, https://doi.org/10.2151/jmsj.2004.597.

Tsuchiya, K., and T. Fujita, 1967: A satellite meteorological study of evaporation and cloud formation over the western Pacific under the influence of the winter monsoon. *J. Meteor. Soc. Japan*, **45**, 232–250, https://doi.org/10.2151/jmsj1965.45.3_232.

Veals, P. G., and W. J. Steenburgh, 2015: Climatological characteristics and orographic enhancement of lake-effect precipitation east of Lake Ontario and over the Tug Hill Plateau. *Mon. Wea. Rev.*, **143**, 3591–3609, https://doi.org/10.1175/MWR-D-15-0009.1.

——, ——, and L. S. Campbell, 2018: Factors affecting the inland and orographic enhancement of lake-effect precipitation over the Tug Hill Plateau. *Mon. Wea. Rev.*, **146**, 1745–1762, https://doi.org/10.1175/MWR-D-17-0385.1.

——, ——, S. Nakai, and S. Yamaguchi, 2019: Factors affecting the inland and orographic enhancement of sea-effect snowfall in the Hokuriku region of Japan. *Mon. Wea. Rev.*, **147**, 3121–3143, https://doi.org/10.1175/MWR-D-19-0007.1.

Villani, J. P., M. L. Jurewicz Sr., and K. Reinhold, 2017: Forecasting the inland extent of lake effect snow bands downwind of Lake Ontario. *J. Oper. Meteor*, **5**, 53–70, https://doi.org/10.15191/nwajom.2017.0505.

West, T. K., W. J. Steenburgh, and G. G. Mace, 2019: Characteristics of sea-effect clouds and precipitation over the Sea of Japan region as observed by A-Train satellites. *J. Geophys. Res. Atmos.*, **124**, 1322–1335, https://doi.org/10.1029/2018JD029586.

Yamada, Y., M. Murakami, H. Mizuno, M. Maki, S. Nakai, and K. Iwanami, 2010: Kinematic and thermodynamical structures of longitudinal-mode snow bands over the Sea of Japan during cold-air outbreaks. Part I: Snow bands in large vertical shear environment in the band-transverse direction. *J. Meteor. Soc. Japan*, **88**, 673–718, https://doi.org/10.2151/jmsj.2010-404.

Yamaguchi, S., O. Abe, S. Nakai, and A. Sato, 2011: Recent fluctuations of meteorological and snow conditions in Japanese mountains. *Ann. Glaciol.*, **52**, 209–215, https://doi.org/10.3189/172756411797252266.

——, K. Iwamoto, and S. Nakai, 2013: Interannual fluctuations of the relationship between winter precipitation and air temperature in the heavy-snowfall zone of Japan. *Ann. Glaciol.*, **54**, 183–188, https://doi.org/10.3189/2013AoG62A302.

Yang, C., Z. Y. Tao, and Z. C. Li, 2009: Overview of research on ocean (lake)-effect snow (in Chinese). *Mar. Sci. Bull*, **28**, 81–88.

Yoshihara, H., M. Kawashima, K. Arai, J. Inoue, and Y. Fujiyoshi, 2004: Doppler radar study on the successive development of snowbands at a convergence line near the coastal region of the Hokuriku District. *J. Meteor. Soc. Japan*, **82**, 1057–1079, https://doi.org/10.2151/jmsj.2004.1057.

Yoshino, M. M., 1977: The winter monsoon. *The Climate of Japan*, E. Fukui, Ed., Elsevier, 65–84.

Zhou, S., M. H. Cong, Z. M. Wu, S. L. Yan, C. F. Yang, and J. J. Zhu, 2008: Characteristics and maintaining mechanisms of sustained cold-air outbreak snowstorms processes in Shandong Peninsula during December 3–21, 2005 (in Chinese). *J. Appl. Meteor. Sci.*, **19**, 444–453.